

A Ditopic O_4S_2 Macrocycle and Its Hard, Soft, and Hard/Soft Metal Complexes Exhibiting Endo-, Exo-, or Endo/Exocyclic Coordination: Synthesis, Crystal Structures, NMR Titration, and Physical Properties

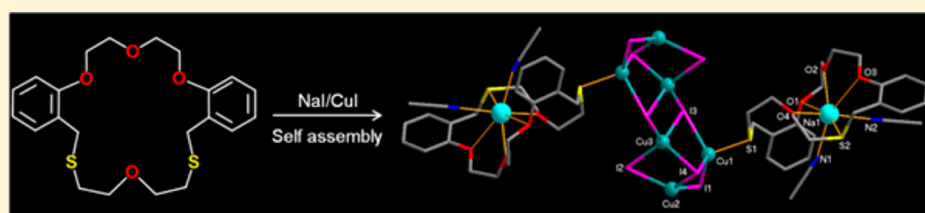
Hyunsoo Ryu,[†] Ki-Min Park,[†] Mari Ikeda,[‡] Yoichi Habata,[§] and Shim Sung Lee^{*,†}

[†]Department of Chemistry and Research Institute of Natural Science, Gyeongsang National University, Jinju 660-701, South Korea

[‡]Education Center, Faculty of Engineering, Chiba Institute of Technology, 2-1-1 Shibazono, Narashino, Chiba 275-0023, Japan

[§]Department of Chemistry, Faculty of Science, Toho University, 2-2-1 Miyama, Funabashi, Chiba 261-0013, Japan

Supporting Information



ABSTRACT: A 20-membered O_4S_2 macrocycle (L^2) was synthesized as a ditopic ligating system toward hard and soft metal ions simultaneously. Five complexes (3–7) of L^2 with different structures and coordination modes, including discrete to infinite forms, mono- to heteronuclear, and endo- to exo- and endo/exocoordination, were prepared and structurally characterized. First, the reaction of L^2 with $Pb(ClO_4)_2 \cdot 3H_2O$ afforded a typical endocyclic mononuclear perchlorato complex $[Pb(L^2)(ClO_4)_2]$ (3) in which one lead(II) is surrounded by the macrocycle adopting a “tight and bent” conformation. Meanwhile, the reaction with a softer metal salt $AgNO_3$ resulted in the formation of the dinuclear bis(macrocycle) complex $[Ag_2(L^2)_2(NO_3)_2]$ (4) in which two exocyclic silver(I) ions are doubly linked by two nitrate ions. The treatment of L^2 with CuI gave a mixture of the exocyclic monomer complex $[Cu(L^2)I]$ (5) and the exocyclic dimer complex $[(Cu_2I_2)(L^2)_2]$ (6), which were separated manually because of their brick and rhomboid shapes of the crystals, respectively. Furthermore, the reaction of L^2 with a mixture of CuI and NaI afforded a photoluminescent heteronuclear complex $[Na_2(Cu_6I_8)(L^2)_2(CH_3CN)_4]_n$ (7) in the endo/exocyclic coordination mode. In this case, the endocyclic sodium(I) complex units are linked by the double-open cubanes-type cluster Cu_6I_8 , yielding a two-dimensional network. The structural and binding properties of the complex of L^2 with silver(I) nitrate in solution were monitored by the NMR titration. Photophysical and thermal properties for complex 7 were also investigated and discussed.

INTRODUCTION

Because of the selective complexation through the central cavity and the self-assembly toward the specific guest, macrocyclic ligands have long been employed as a key species in supramolecular coordination chemistry.¹ Recently, much progress in macrocyclic supramolecular chemistry has been made in regard to the heteronuclear and coordination network systems.² In other words, by selecting appropriate metal species, counterions, clusters, as well as donor arrangement in the macrocyclic host, the coordination mode and connectivity patterns of the resulting products can be rationally controlled.^{2,3} For instance, a crown-type macrocycle forms stable complexes where the metal ion locates inside the cavity (endocyclic coordination). However, a sulfur-containing macrocycle (or thiamacrocycle) prefers an exocyclic coordination so often because of the propensity of sulfur atoms to orient toward the outside the cavity.⁴

Synthetically, the exocoordination could be advantageous because it often induces the formation of more exquisite networks than could be possible to prepare through the

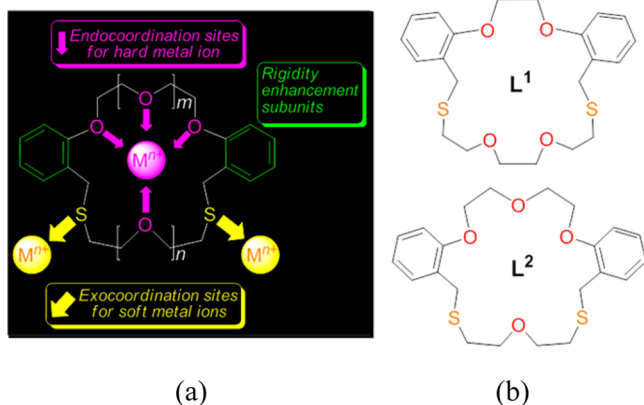
endocoordination.^{2,5,6} So, the exocoordination can also be used in crystal engineering as a versatile tool. For the stable host–guest complexation of a given macrocycle, besides the choice of metal cation, other controlling factors such as anion,^{3c,7} solvent,⁸ and coligand⁹ are important. Diverse types of supramolecular structures and coordination modes for the thiamacrocycle complexes, including mono- to multinuclear, discrete and infinite forms, as well as the endo- and exocyclic systems have been introduced^{3–10} and reviewed.²

Recently, our group introduced the homo- and heteronuclear polymeric networks linked with different types of CuI clusters obtained from the assembly reaction of a ditopic O_4S_2 macrocycle L^1 (Scheme 1b) with CuI in the absence and presence of KI .¹¹ In the former case, an emissive one-dimensional (1D) species linked with the cubane CuI cluster was isolated. In the latter case, however, the mixture of CuI and KI induced the endocoordination of L^1 toward K^+ and the

Received: December 12, 2013

Published: April 9, 2014

Scheme 1. (a) Concept of Ditopic Oxathia Macrocycles for Endo/Exo-Coordination Modes and (b) O_4S_2 Macrocyclic Isomers L^1 and L^2



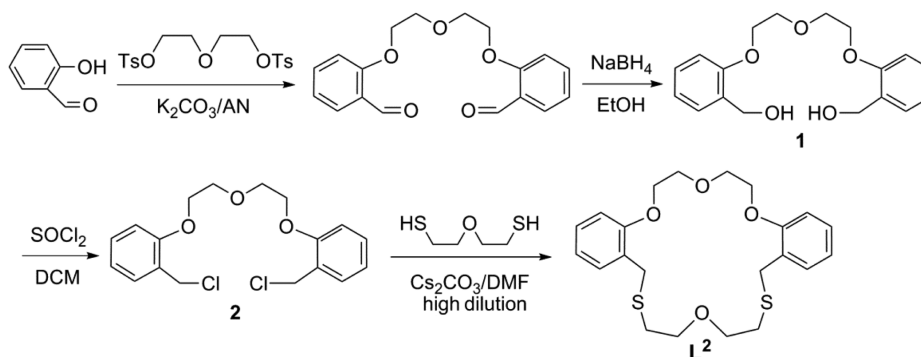
rearrangement of the ribbon-type CuI cluster in the exocyclic mode.

As an extension of the above investigations, we focused our attention not only on the new thiophilic metal complex system of thiamacrocycles but also on a hard/soft heteronuclear complex species that would potentially influence the endo- and exocyclic coordination modes as well as networking (Scheme 1a). In particular, we are interested in extending this area by using a new ditopic O_4S_2 macrocycle L^2 , which is a regioisomer of L^1 (Scheme 1b). In the present study, we report the synthesis of L^2 as a potent ditopic ligand, its hard and soft metal complexes, as well as a soft/hard heterometallic complex of it. For example, following the formation of one endocyclic hard metal complex and two soft metal exocyclic complexes, the preparation and structural characterization of the endo/exocyclic complex linked by CuI cluster adopting a double-open cubane¹² was proved possible.

RESULTS AND DISCUSSION

Synthesis of the O_4S_2 Macrocyclic L^2 . Synthesis of the target macrocycle L^2 began with salicylaldehyde (Scheme 2). Dichloride precursor **2** for the cyclization was prepared through the chlorination of dialcohol **1**, which obtained from the reduction of dialdehyde.¹³ The macrocycle L^2 was synthesized from the coupling cyclization between dichloride **2** and 2-mercaptoethyl ether in the presence of Cs_2CO_3 under high dilution condition in a reasonable yield.

Scheme 2. Synthesis of L^2



Preparation of Supramolecular Complexes with L^2 . Five complexes (3–7) of L^2 whose structures depend on the coordination modes of L^2 toward lead(II), silver(I), copper(I), and sodium(I) salts were synthesized and structurally characterized as depicted in Scheme 3. The resulting X-ray crystal structures are shown in Figures 1–4, with X-ray data and selected geometric parameters presented in Tables 1–6.

Endocyclic Monolead(II) Complex (3). The reaction of L^2 with $Pb(ClO_4)_2 \cdot 3H_2O$ in acetonitrile/dichloromethane yielded colorless crystalline product **3**. The X-ray analysis revealed that **3** is a 1:1 (metal-to-ligand) complex $[Pb(L^2)(ClO_4)_2]$. The lead(II) is eight-coordinate in the macrocyclic cavity, and the metal center is bound to all donor atoms of L^2 , adopting a “tight and bent” conformation. The coordination sphere of the metal center is completed by two O atoms from the two monodentate perchlorate ions in both sides of the macrocyclic plane. The coordination geometry can best be described as a distorted hexagonal bipyramid with the O_4S_2 donors of L^2 defining the hexagonal plane and the axial positions occupied by two O atoms of two perchlorato ligands. Because of the $Pb1 \cdots O6$ interaction [2.975(13) Å, dashed lines in Figure 1], the $O5-Pb1-O9$ angle [147.8(4)°] is highly distorted from the linearity, and the $Pb1-O5$ bond distance [2.751(11) Å] is fairly elongated. Among the $Pb-O_{ether}$ bond distances, the $Pb1-O4$ bond [2.930(8) Å] is longer than others [2.674(9)–2.838(8) Å] due to its isolated location between heterodons. The $Pb-S$ bond lengths [$Pb1-S1$ 2.866(3), $Pb1-S2$ 2.936(3) Å] are within the normal range for this bond type.¹⁴ The preference for the endocyclic mononuclear complex formation may be associated with the intermediate nature of the lead(II) between soft and hard acids.¹⁵

Exocyclic Silver(I) Nitrate Complex (4). Considering the sulfur donors as a soft base, silver(I) nitrate was employed and treated with L^2 to yield the colorless complex **4** (Figure 2). Unlike **3**, complex **4** is a dinuclear bis(macrocycle) complex with formula $[Ag_2(L^2)_2(NO_3)_2]$. Further, the two crystallographically equivalent Ag atoms locate outside the macrocyclic cavity in a bent conformation exhibiting an exocyclic coordination mode. In the dimeric structure of **4**, the two Ag atoms are doubly linked by the two coordinating nitrate ions, forming a $Ag-(\mu_2-NO_3)_2-Ag$ square unit¹⁶ sandwiched by two macrocycles. The Ag atom is five-coordinate, being bound by OS_2 donors from one L^2 , with the remaining three oxygen donors between two benzo units uncoordinated. The coordination sphere is completed by two monodentate nitrate ligands bridging two Ag atoms. The $Ag-S$ bond distances [2.5147(5), 2.5235(5) Å] in **4** are typical, while the $Ag1-O4$

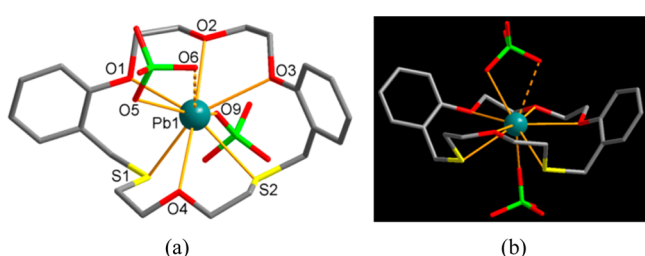
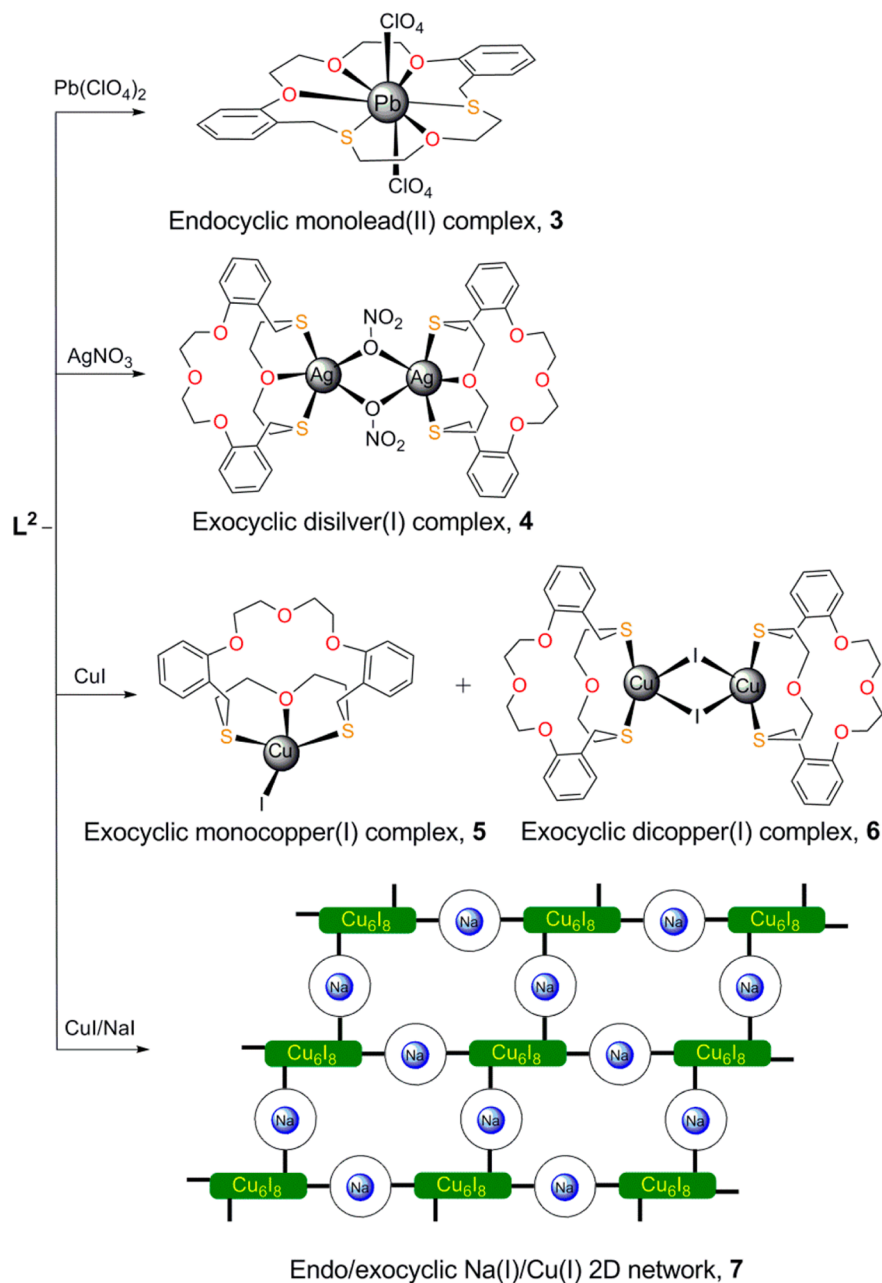
Scheme 3. Complexes of L^2 with Different Coordination Modes

Figure 1. Endocyclic monolead(II) complex **3**, $[\text{Pb}(\text{L}^2)(\text{ClO}_4)_2]$: (a) top view and (b) side view. Hydrogen atoms are omitted.

bond distance [2.7608(14) Å] is also within the normal literature range for this bond type.¹⁷ The $\text{Ag}\cdots\text{Ag}$ separation in **4** is 3.986 Å. We have reported some coordination polymers of thiamacrocycles linked by the $\text{Ag}-(\mu_2\text{-NO}_3)_2\text{-Ag}$ square unit adopting one-dimensional (1D) and two-dimensional (2D)

structures.^{16a} To the best of our knowledge, **4** is the first characterized example of the discrete type, in which macrocycles are linked by such square unit.

Exocyclic Copper(I) Iodide Complexes (5 and 6). Having obtained the lead(II) and silver(I) complexes of L^2 in the endo- and the exocoordination modes, respectively, we have proceeded to the preparation of the complexes by employing copper(I) iodide as an example of thiophilic soft metal species. As is well-known, the self-assembly of copper(I) iodide with multidentate soft base ligands often leads to discrete complexes and continuous ones because the copper(I) halides are capable of adopting a variety of structural motifs such as rhomboid dimer, cubane tetramer, hexagonal prism, double cubanes, 1D chain, double-stranded stairs, and more (Scheme 4).¹⁸ Such CuI clusters exhibit an unusual wealth of stoichiometries and geometries because of the small energy

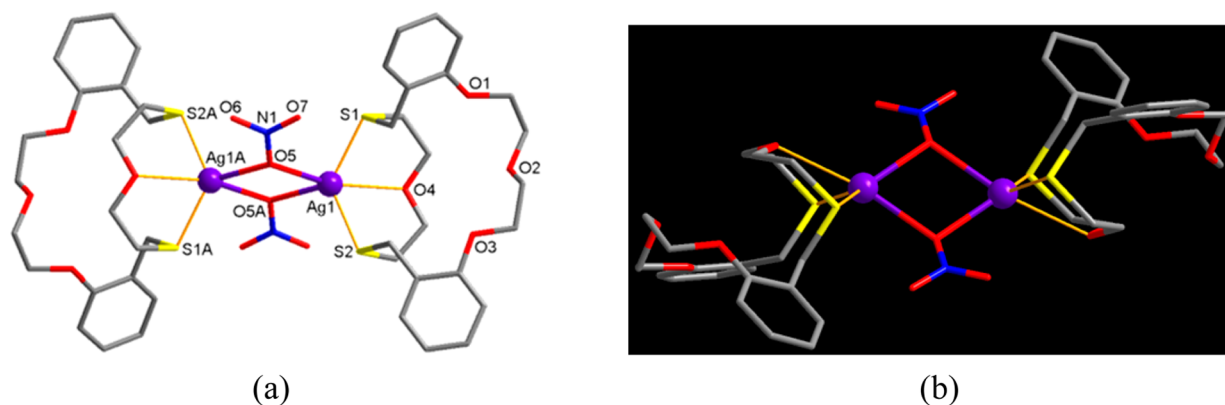


Figure 2. Exocyclic silver(I) nitrate complex **4**, $[\text{Ag}_2(\text{L}^2)_2(\text{NO}_3)_2]$: (a) top view and (b) side view. Hydrogen atoms are omitted.

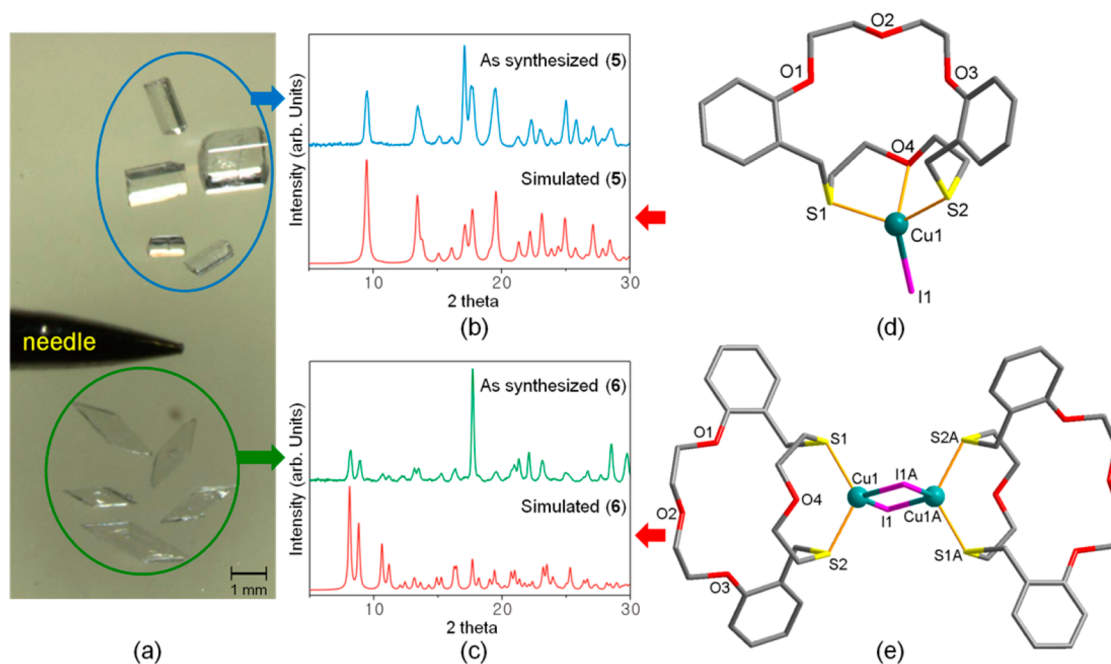


Figure 3. (a) Photomicroscope of a mixture of brick-shaped (**5**) and rhomboid-shaped (**6**) single crystals after the manual separation with a needle under microscope, (b) PXRD data of **5**, (top) as synthesized and (bottom) simulated, (c) PXRD data of **6**, (top) as synthesized and (bottom) simulated, (d) crystal structure of **5**, $[\text{Cu}(\text{L}^2)\text{I}]$, and (e) crystal structure of **6**, $[(\text{Cu}_2\text{I}_2)(\text{L}^2)_2]$.

difference between the polymorphs, which are prepared depending on synthetic conditions.

As shown in Figure 3a, the reaction of L^2 with copper(I) iodide in acetonitrile afforded a mixture of two products, which can be identified by naked eyes. In fact, the colorless crystalline product shows two crystal shapes (or crystal habits): brick and rhomboid (later compounds **5** and **6**, respectively). As mentioned, this seems to be the case for the product, which contains a mixture of two species. No crystals except those with either shape exist in the product. So it was possible to separate these two types of crystals using a needle manually under the microscope. As expected, the single-crystal X-ray analysis revealed that the observed difference in the crystal habit means different species. For example, the brick-shaped one (**5**) and rhomboid-shaped one (**6**) crystallize with space groups $P2_1/m$ and $P2_1/c$, respectively (Figure 3). Also the agreement between the powder X-ray diffraction (PXRD) patterns of each manually separated product and the simulated patterns for the corresponding single crystals indicates that two species are effectively separated, showing the bulk purity (Figure 3b,c).

The crystal structures of **5** and **6** are shown in Figure 3d,e, respectively, and their selected geometric parameters are presented in Tables 4 and 5. First, the crystal analysis confirms that **5** is a half-sandwich type 1:1 (metal-to-ligand) complex $[\text{Cu}(\text{L}^2)\text{I}]$. The Cu(I) center in **5** is coordinated by OS_2 donors from L^2 in a folded conformation, with the fourth coordination site occupied by one iodo ligand. The coordination sphere of the metal center is distorted tetrahedral, with the bond angles ranging from $83.49(10)^\circ$ for $\text{S1A}-\text{Cu1}-\text{O4}$ to $125.54(9)^\circ$ for $\text{S1}-\text{Cu1}-\text{S1A}$. The three oxygen donors (O1, O2, and O3) between two benzo units remain uncoordinated.

Meanwhile, **6** crystallized as a 2:2 complex $[(\text{Cu}_2\text{I}_2)(\text{L}^2)_2]$, with two macrocycles sandwiching an exodentate rhomboid dimer cluster, Cu_2I_2 (see Scheme 4a). In **6**, each Cu atom that lies outside the macrocyclic cavity is also four-coordinate, being bound to two S donors from one macrocycle and the two bridging I atoms. Two Cu centers are then linked by two μ_2 -I atoms, forming a rhomboid, with all O atoms of the macrocycle remaining uncoordinated. The coordination geometry around each Cu center is considerably distorted from regular

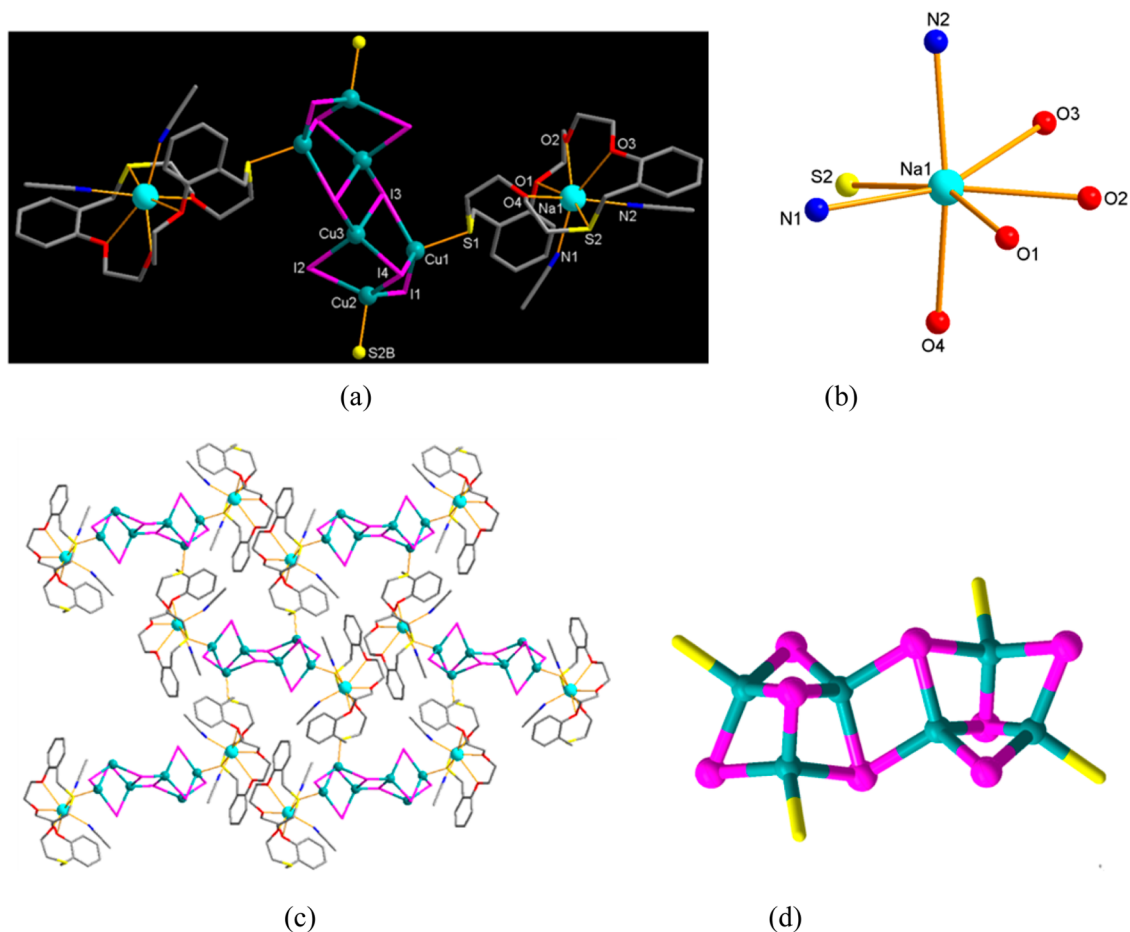


Figure 4. Endo/exocyclic coordination polymer 7, $[\text{Na}_2(\text{Cu}_6\text{I}_8)(\text{L}^2)_2(\text{CH}_3\text{CN})_4]_n$: (a) basic coordination unit, (b) coordination environment of endocyclic Na1 atom showing a distorted pentagonal bipyramid geometry, (c) 2D brick-wall type network structure, and (d) double-open cubanes unit Cu_6I_8 .

Table 1. Crystallographic Data and Structure Refinement for Complexes 3–7

	3	4	5	6	7
formula	$\text{C}_{22}\text{H}_{28}\text{Cl}_2\text{O}_{12}\text{PbS}_2$	$\text{C}_{44}\text{H}_{54}\text{Ag}_2\text{N}_2\text{O}_{14}\text{S}_4$	$\text{C}_{22}\text{H}_{28}\text{CuI}_8\text{O}_4\text{S}_2$	$\text{C}_{44}\text{H}_{56}\text{Cu}_2\text{I}_8\text{O}_8\text{S}_4$	$\text{C}_{26}\text{H}_{34}\text{Cu}_3\text{I}_4\text{N}_2\text{NaO}_4\text{S}_2$
formula weight	826.65	1178.87	611.00	1222.01	1223.88
temperature (K)	173(2)	173(2)	173(2)	173(2)	173(2)
crystal system	monoclinic	monoclinic	monoclinic	monoclinic	monoclinic
space group	Pc	$P2_1/c$	$P2_1/m$	$P2_1/c$	$P2_1/c$
Z	2	2	2	2	4
a (Å)	8.7113(3)	9.74720(10)	6.86320(10)	9.1904(6)	12.4226(6)
b (Å)	10.0389(3)	19.4245(3)	18.5960(3)	20.0371(14)	20.6183(9)
c (Å)	17.8182(5)	14.5507(2)	9.3849(2)	15.1204(9)	18.4739(6)
α (deg)	90	90	90	90	90
β (deg)	118.193(2)	118.4270(10)	97.2890(10)	120.884(4)	129.865(2)
γ (deg)	90	90	90	90	90
V (Å ³)	1373.37(7)	2422.77(6)	1188.10(4)	2389.6(3)	3631.9(3)
D_x (g/cm ³)	1.999	1.616	1.708	1.698	2.238
$2\theta_{\text{max}}$ (deg)	52	52	52	52	52
R_1, wR_2 [$I > 2\sigma(I)$]	0.0478, 0.1301	0.0233, 0.0547	0.0498, 0.1261	0.0203, 0.0558	0.0219, 0.0448
R_1, wR_2 [all data]	0.0507, 0.1332	0.0274, 0.0567	0.0514, 0.1271	0.0216, 0.0573	0.0273, 0.0465
GOF	1.081	1.038	1.467	1.031	1.057
data/restraints/parameters	4205/2/352	4737/6/298	2426/18/142	4703/8/272	7135/0/381
no. of reflection used [$>2\sigma(I)$]	4205 [$R_{\text{int}} = 0.0561$]	4737 [$R_{\text{int}} = 0.0285$]	2426 [$R_{\text{int}} = 0.0246$]	4703 [$R_{\text{int}} = 0.0448$]	7135 [$R_{\text{int}} = 0.0355$]
structure determination	SHELXTL	SHELXTL	SHELXTL	SHELXTL	SHELXTL
refinement	full-matrix	full-matrix	full-matrix	full-matrix	full-matrix

Table 2. Selected Bond Lengths (Å) and Bond Angles (deg) for Complex 3

Pb1–S1	2.866(3)	Pb1–S2	2.936(3)
Pb1–O1	2.810(8)	Pb1–O2	2.674(9)
Pb1–O3	2.838(8)	Pb1–O4	2.930(8)
Pb1–O5	2.751(11)	Pb1–O9	2.495(10)
S1–Pb1–S2	82.09(9)	S1–Pb1–O1	71.26(18)
S1–Pb1–O2	126.15(19)	S1–Pb1–O3	147.11(19)
S1–Pb1–O5	92.5(2)	S1–Pb1–O9	75.2(3)
S2–Pb1–O1	147.87(19)	S2–Pb1–O2	127.2(2)
S2–Pb1–O3	72.04(18)	S2–Pb1–O5	127.6(3)
S2–Pb1–O9	80.8(3)	O1–Pb1–O2	62.2(2)
O1–Pb1–O3	123.8(2)	O1–Pb1–O5	72.4(3)
O1–Pb1–O9	75.4(3)	O2–Pb1–O3	61.8(2)
O2–Pb1–O5	97.7(3)	O2–Pb1–O9	68.5(3)
O3–Pb1–O5	119.3(3)	O3–Pb1–O9	80.8(3)
O5–Pb1–O9	147.8(4)		

Table 3. Selected Bond Lengths (Å) and Bond Angles (deg) for Complex 4

Ag1–S1	2.5235(5)	Ag1–S2	2.5147(5)
Ag1–O4	2.7608(14)	Ag1–O5	2.5161(14)
Ag1–O5A	2.3900(14)		
S1–Ag1–S2	125.411(17)	S1–Ag1–O4	73.86(3)
S1–Ag1–O5	112.61(4)	S1–Ag1–O5A	104.69(4)
S2–Ag1–O4	72.54(3)	S2–Ag1–O5	93.23(4)
S2–Ag1–O5A	129.42(4)	O4–Ag1–O5	165.05(4)
O4–Ag1–O5A	121.14(4)	O5–Ag1–O5A	71.34(5)

Table 4. Selected Bond Lengths (Å) and Bond Angles (deg) for Complex 5

Cu1–S1	2.2677(17)	Cu1–S1A	2.2677(17)
Cu1–O4	2.356(7)	Cu1–I1	2.5199(9)
S1–Cu1–S1A	125.54(9)	S1–Cu1–O4	83.49(10)
S1A–Cu1–O4	83.49(10)	S1–Cu1–I1	116.74(4)
S1A–Cu1–I1	116.74(4)	O4–Cu1–I1	114.83(19)

Table 5. Selected Bond Lengths (Å) and Bond Angles (deg) for Complex 6

Cu1–S1	2.3247(6)	Cu1–S2	2.3234(5)
Cu1–I1	2.7377(3)	Cu1–I1A	2.5871(3)
S1–Cu1–S2	121.977(19)	S1–Cu1–I1	106.562(16)
S1–Cu1–I1A	102.416(16)	S2–Cu1–I1	91.377(15)
S2–Cu1–I1A	118.766(15)	I1–Cu1–I1A	115.465(9)

tetrahedral, with the bond angles ranging from 91.377(15)° for S2–Cu1–I1 to 121.977(19)° for S2–Cu1–S1. The Cu...Cu distance (2.846 Å) in **6** is slightly longer than the sum of the van der Waals radii (2.80 Å).¹⁹ Several dimeric copper(I) halide complexes of thiamacrocycles with similar structures have been previously reported by us.²⁰

The overall conformational difference between **5** and **6** in the exocoordination mode originates mainly from the monomer and the dimer arrangement. Accordingly, the coordination environment of each copper(I) center in both compounds is more or less different. For example, the Cu1–O4 [2.356(7) Å] in **5** is consistent with typical strong coordination to the copper center; however, the Cu1...O4 [2.997(2) Å] in **6** shows fairly elongated distance due to the two Cu1–I bond formation for the dimerization.

Table 6. Selected Bond Lengths (Å) and Bond Angles (deg) for Complex 7

Cu1–S1	2.337(1)	Cu1–I1	2.615(1)
Cu1–I3	2.706(1)	Cu1–I4	2.636(1)
Cu2–S2B	2.325(1)	Cu2–I1	2.666(1)
Cu2–I2	2.640(1)	Cu2–I4	2.689(1)
Cu3–I2	2.643(1)	Cu3–I3	2.669(1)
Cu3–I3A	2.638(1)	Cu3–I4	2.738(1)
Na1–S2	2.883(1)	Na1–O1	2.837(3)
Na1–O2	2.374(2)	Na1–O3	2.953(3)
Na1–O4	2.373(2)	Na1–N1	2.416(3)
Na1–N2	2.396(4)		
S1–Cu1–I1	111.6(1)	S1–Cu1–I3	100.0(1)
S1–Cu1–I4	108.6(1)	I1–Cu1–I3	106.8(2)
I1–Cu1–I4	114.5(2)	I3–Cu1–I4	114.5(2)
S2B–Cu2–I1	105.2(1)	S2B–Cu2–I2	107.1(1)
S2B–Cu2–I4	105.3(1)	I1–Cu2–I2	112.5(2)
I1–Cu2–I4	111.1(2)	I2–Cu2–I4	114.8(2)
I2–Cu3–I3	107.1(2)	I2–Cu3–I4	113.1(2)
I3–Cu3–I4	112.3(2)	I3A–Cu3–I4	99.1(2)
I3A–Cu3–I2	114.1(2)	I3A–Cu3–I3	111.0(2)
S2–Na1–N1	83.1(1)	S2–Na1–O3	71.2(1)
O1–Na1–O2	62.3(1)	O1–Na1–N1	82.3(1)
O2–Na1–O3	64.0(1)	O4–Na1–N2	161.0(1)

Endo/Exocyclic Heteronuclear Na(I)/Cu(I) Network Complex (7). As proposed in Scheme 1, we also examined the ditopic behaviors of **L**², employing the mixture of hard and soft metal iodides to isolate the heterometallic complexes with an endo/exocyclic coordination. Among the mixed system of the metal salts, when a mixture of NaI and CuI was used in the reactions of **L**², colorless crystalline product **7** suitable for X-ray analysis was obtained.

X-ray analysis revealed that **7** is a 2D network complex [Na₂(Cu₆I₈)(L²)₂(CH₃CN)₄]_n, involving heterometallic Na(I)/Cu(I) ions, in which the two different metal ions are positioned inside and outside the cavity (Figure 4). The purity of the bulk product **7** was also confirmed by comparing the simulated PXRD patterns from the single-crystal data with those from the bulk sample (Figure 5). The gross 2D architecture for **7** can be considered as an infinite brick-wall pattern (Scheme 3 and Figure 4c). And the asymmetric unit for **7** contains one L², one Na atom, two acetonitrile molecules, three Cu atoms, and four I atoms. The single brick unit for **7** contains four asymmetric units, with each macrocycle being linked by a Cu₆I₈ unit.

The Na atom in the macrocyclic cavity is seven-coordinate, with the coordination to four O atoms and one S atom from L² in a twisted arrangement (Figure 4a). The remaining two sites are occupied by two acetonitrile molecules in one side of the macrocyclic plane. The sodium(I) coordination in **7** can be described as a distorted pentagonal bipyramidal geometry, where O1, O2, O3, S2, and N1 atoms form the pentagonal plane, while N2 and O4 atoms occupy the axial positions [N2–Na1–O4 161.0(1)°] (Figure 4b). The bite angles between two adjacent donors on the pentagonal plane vary from 62.3(1) to 83.1(1)°. Some of the Na–O bonds [Na1–O1 2.837(3), Na1–O3 2.953(3) Å] show elongated lengths because of the larger macrocyclic cavity size for the sodium(I) complexation. Other Na–O bond distances [2.373(2)–2.396(4) Å] are typical. The Na1–S2 length [2.883(1) Å] is shorter than the sum of the van der Waals radii (2.30 + 1.80 Å),¹⁹ suggesting that the S atom is a weaker donor for the endocyclic coordination of sodium(I).

Scheme 4. Representation of Some CuI Clusters

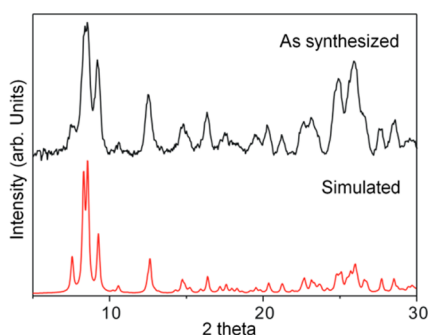
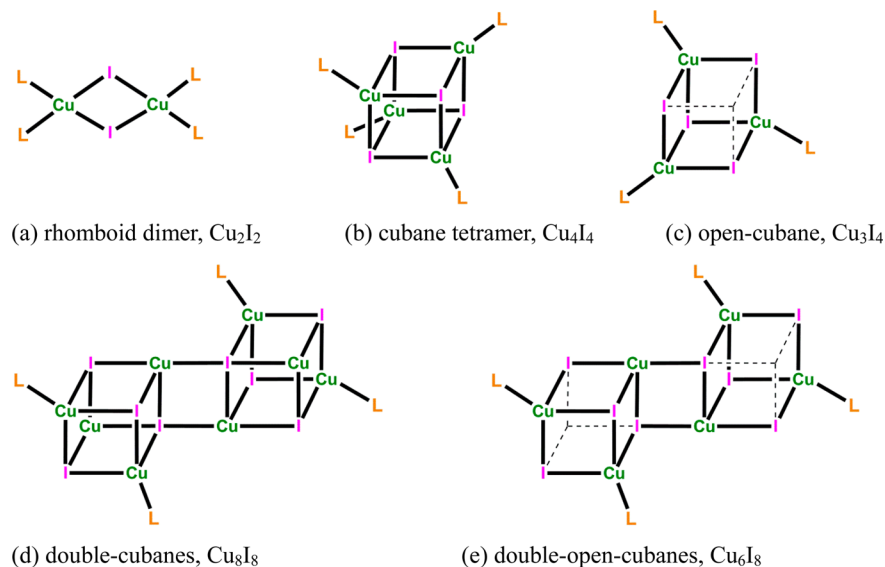


Figure 5. PXRD patterns for complex 7: (top) as synthesized and (bottom) simulated from the single-crystal X-ray data.

Notably, the S1 atom coordinates not to the Na(I) center [$\text{Na1}\cdots\text{S1}$ 4.370(2) Å] but to the Cu1 atom [$\text{Cu1}\cdots\text{S1}$ 2.337(1) Å] in an exocoordination mode to form a 2D network. In 7, there are three crystallographically independent Cu atoms (Cu1, Cu2, and Cu3) linked by four I atoms, forming a double-open cubanes cluster Cu_6I_8 that acts as a planar four-connecting node (see Scheme 4e and Figure 4d). The Cu_6I_8 motif, in which two open-cubane²¹ Cu_3I_4 units are doubly linked via Cu–I bonds, is constructed from six Cu, four μ_2 -I, and four μ_3 -I atoms. Thus, the double-open cubane motif can be regarded as the deformation of the normal double cubanes²² clusters by removing three Cu–I bonds located at the same corner (the dashed lines in Scheme 4e) of each cubane tetramer. Each Cu_6I_8 unit is connected by four macrocyclic ligands in a trans conformation, generating a brick-wall type 2D (4,4) layer with a single brick containing four macrocycles and four Cu_6I_8 clusters with a dimension of ca. 20×30 Å². Until now only two compounds with the double-open cubanes-type Cu_6I_8 cluster have been reported by Sheldrick^{12a} and our group.^{12b} Thus, to our knowledge, 7 is the third example. Consequently, sodium(I) iodide induces not only the endocyclic cation complexation of the macrocycle but also the formation of the negatively charged double-open cubanes-type copper(I) iodide cluster, which generates the 2D network structure via the exocyclic coordination.

Physical Properties of the Complexes. Since the photoluminescence behaviors of copper(I) halide clusters for such thiamacrocyclic complexes is highly dependent on their structures,^{18,23} the photoluminescence spectra of the above products were measured in the solid state. As mentioned above, two cases of the compounds involving the double-open cubanes Cu_6I_8 have been reported.¹² However, note that no photoluminescence properties of those complexes have been reported so far, in contrast to the cubane tetramer Cu_4I_4 complexes showing the well-explored photoluminescence behaviors.^{20a,b,24}

Upon excitation at 365 nm, however, complex 7 in the solid state exhibits a weak yellow-green emission with a maximum at 418 nm dominated by a high-energy band (HE, Figure 6). The

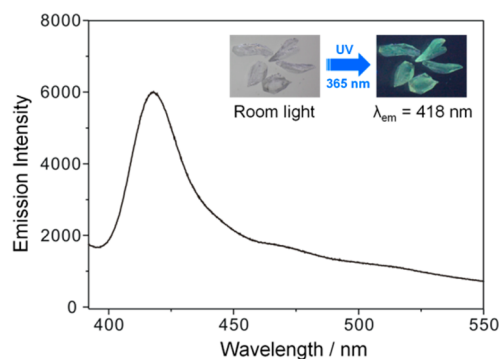


Figure 6. Solid-state photoluminescence spectrum of complex 7 at room temperature (excitation at 365 nm).

absolute quantum yield for 7 in the solid state at 365 nm in room temperature was determined to be $\Phi = 0.01$. The emission of 7 presented may be assigned to a triplet halide-to-ligand charge transfer (XLCT) excited state.²⁵ In the cubane tetramer Cu_4I_4 complex, the emissions observed around 550 nm at room temperature are dominated by the low-energy band (LE: XMCT/CC) while, at low temperature, the emissions around 420 nm are dominated by a high energy one (HE: XLCT).²⁵ As expected, 5 and 6 show no photoluminescence in the solid state.

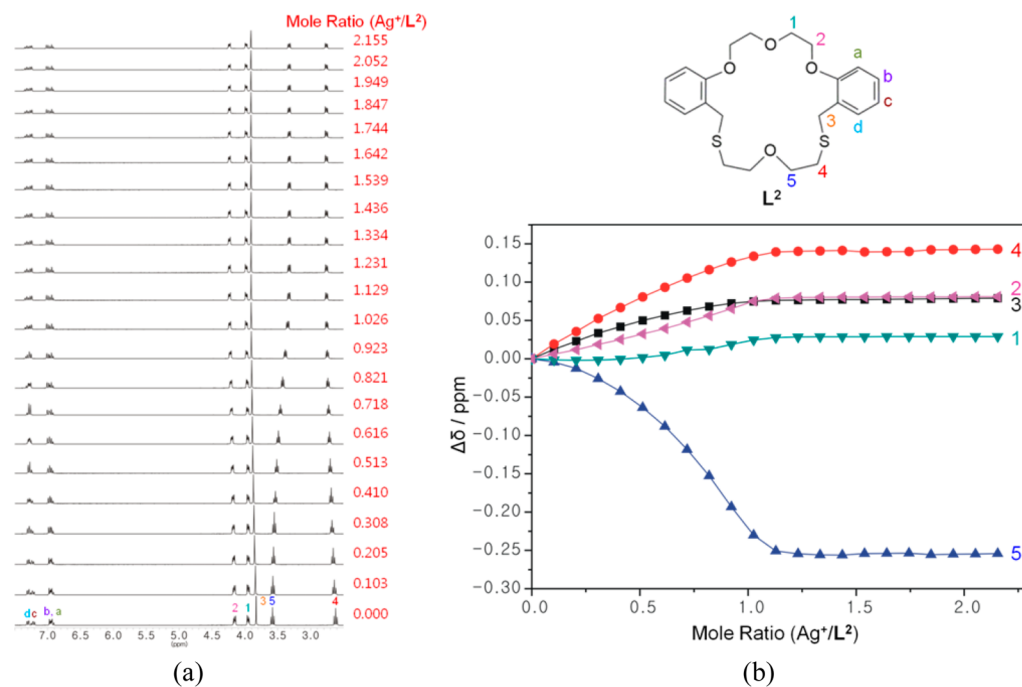


Figure 7. (a) ¹H NMR spectra of L² following the stepwise addition of AgNO₃ in CD₃CN and (b) their titration curves for each proton in L². [L²] = 7.61 × 10⁻³ M, [AgNO₃] = (0–1.39) × 10⁻² M.

Thermogravimetric analysis (TGA) performed on **7** shows a weight loss of 6.48% at around 180 °C, corresponding to the loss of coordinated acetonitrile molecules (expected value 6.71%) (Figure S1 in the Supporting Information). The IR spectrum of **7** obtained after heating to 190 °C also confirms the removal of acetonitrile by the disappearance of the absorption peak at 2268 cm⁻¹ (ν_{CN}). Because single crystallinity was not retained during the removal process of the coordinated acetonitrile by heating, further structural studies were not available.

¹H NMR Study of the Ag(I) Complexation. To obtain information on the complexation behavior in solution, the ¹H NMR titration was carried out. For the titrations of L² with Na⁺ or other alkali metal ions, the cation-induced spectral changes were negligible, suggesting very weak interactions due to the existence of two soft sulfur donors in L². When the metal species was changed to silver(I) nitrate in the titration experiment, it was possible to obtain the meaningful complexation-induced chemical shifts for the ligand exhibiting a typical slow-exchange system (Figure 7).

For the free L², the signals of the aromatic protons (H_{a-d}) and the methylene protons (H₁₋₅) are well-identified (Figure 7a). The cation-induced chemical shift changes (Δδ) were measured on the variation of the mole ratio (Ag⁺/L², 0–2.2 equiv) (Figure 7b). The titration curves show that all the methylene proton signals except H₅ shifted downfield and exhibit no more shifts above a mole ratio (Ag⁺/L²) of 1.0, indicating a 1:1 stoichiometry for the complexation.

The magnitudes of the cation-induced shifts follow the sequence H₅ ≫ H₄ > H₂, H₃ > H₁. The largest shift (toward upfield) for H₅ adjacent to the O donor between two S donors shows the key contribution of this O donor to the coordination is, to some extent, exceptional because the observed chemical shifts for H₁ and H₂ adjacent to other three O donors are much smaller than that for the former one. The second largest shift (toward downfield) for H₄ adjacent to the S donor shows the

contribution of the S donors to the coordination. From these results, the silver(I) ion is mainly stabilized by the –S–O–S– donor set in the flexible segment and the contribution from the –O–O–O– segment is negligible, similar to the result suggested in the solid state.

CONCLUSION

The new O₄S₂-donor macrocycle L² was proposed as a ditopic ligating system toward the hard and soft metal ions simultaneously. The macrocycle L² was synthesized and used to prepare its endocyclic lead(II) complex together with exocyclic silver(I) nitrate and copper(I) iodide complexes. Interestingly, the latter one contains a mixture of one monomer and one dimer complexes, which can be separated manually because of their different shapes of the crystals. The ditopic ligand L² also enabled us to prepare an emissive heteronuclear complex comprising a 2D polymeric network in which the endocyclic heteronuclear [Na(I)/Cu(I)] complex units are linked with double-open cubanes-type copper(I) iodide cluster to form a brick-wall type structure. From these results, it is concluded that by employing the preferred exocyclic coordination mode based on the thiophilicity of soft metals, in association with the endocoordination of the hard metal ions, it is possible to construct the endo/exocyclic heteronuclear network species displaying a considerable degree of sophistication.

EXPERIMENTAL SECTION

General. All chemicals and solvents used in the syntheses were of reagent grade and were used without further purification. The electrospray ionization (ESI) mass spectra were obtained on a Thermo Scientific LCQ Fleet spectrometer. The high resolution mass spectra (HRMS) were obtained on a JEOL JMS-700 spectrometer. NMR spectra were recorded on a Bruker 300 spectrometer (300 MHz). The Fourier transform infrared (FT-IR) spectra were measured with a Nicolet iS10 spectrometer. The elemental analysis was carried out on a LECO CHNS-932 elemental analyzer. The absolute quantum

yield was measured with a Hamamatsu Quantaurus-QY C11347–11 absolute photoluminescence quantum yields measurement system.

Synthesis of Compound 1. To a warm ethanolic solution (100 mL) of dialdehyde (3.0 g, 9.54 mmol) was added NaBH₄ (1.15 g, 30.54 mmol) slowly, and then half of the solvent volume was reduced by boiling the reaction mixture. After this mixture was cooled to room temperature, water (400 mL) was added to precipitate the colorless solid product. IR (KBr, pellet): 3384, 3274 (br, O–H), 2935, 2882 (m, aliphatic C–H), 1603, 1591 (m, aromatic C=C), 1492, 1453 (s, aromatic C=C), 1286 (m), 1239 (s), 1124(m), 1047 (s, C–O), 932(w), 755 (s) cm⁻¹. ¹H NMR (300 MHz, CDCl₃, δ): 6.85–7.27 (m, 8H, aromatic), 4.62 (s, 4H, ArCH₂), 4.21 (t, 4H, ArOCH₂), 3.99 (t, 2H, ArCH₂OH), 3.89 (t, 4H, ArOCH₂CH₂). ¹³C{¹H} NMR (75 MHz, CDCl₃) 156.9, 130.2, 129.6, 129.0, 121.3, 112.2, 69.8, 67.8, 61.8. HRMS (fast atom bombardment (FAB)): Calcd for C₁₈H₂₃O₅ ([M + H]⁺): 319.1545, Found: 319.1553.

Synthesis of Compound 2. To a stirred suspension of compound 1 (2.00 g, 6.3 mmol) in dichloromethane (100 mL) was added thionyl chloride (2.99 g, 25 mmol) dropwise. The reaction mixture was maintained for 4 h. Ethanol (95%, 5 mL) was added carefully, and the reaction mixture stirred at room temperature for a further 2 h. The solvent was evaporated to yield a light yellow oil. Water (100 mL) was added, and the mixture was extracted with dichloromethane (3 × 100 mL). The organic phase was dried over anhydrous sodium sulfate and filtered, and the solvent was removed to yield a yellow oil (2.18 g) in 98% yield. IR (KBr, pellet): 3082, 3037 (m, aromatic C–H), 2924, 2885 (m, aliphatic C–H), 1603, 1588 (m, aromatic C=C), 1495, 1450 (s, aromatic C=C), 1262, 1249 (s, CH₂–Cl), 1132–1047 (m, C–O), 959 (m), 828 (m), 753 (s, C–Cl), 659 (m) cm⁻¹. HRMS (EI) Calcd for C₁₈H₂₀Cl₂O₃ (M⁺): 354.0789. Found: 354.0794. ¹H NMR (300 MHz, CDCl₃, δ): 6.80–7.28 (m, 8H, aromatic), 4.61 (s, 4H, ArCH₂), 4.08 (t, 4H, ArOCH₂), 3.86 (t, 4H, ArOCH₂CH₂). ¹³C{¹H} NMR (75 MHz, CDCl₃) 156.8, 130.7, 130.2, 126.3, 121.1, 112.3, 70.0, 68.4, 41.8.

Synthesis of L². Cesium carbonate (2.57 g, 7.88 mmol) was dissolved in dimethylformamide (DMF) (1500 mL) in a 3 L round-bottom flask. 2-Mercaptoethyl ether (0.78 g, 5.63 mmol) and dichloride 2 (2.00 g, 5.63 mmol) were dissolved in DMF (100 mL) and placed in a 50 mL glass syringe. The contents of the syringe were added dropwise at a regular rate (0.6 mL h⁻¹) into the Cs₂CO₃–DMF solution under a nitrogen atmosphere with the aid of a micro-processor-controlled syringe pump at 55–60 °C over 50 h. The mixture was allowed to stand for a further 10 h. After it was cooled to room temperature, the reaction mixture was filtered, and the solvent was evaporated. Water (100 mL) was added, and the mixture was extracted with dichloromethane. The organic phase was dried over anhydrous sodium sulfate and filtered, and the solvent was removed to give a yellow oil. Flash column chromatography (SiO₂, *n*-hexane/ethyl acetate 8:2) afforded the final product L² as a colorless solid in 43% yield. For L², mp 88–90 °C. IR (KBr, pellet): 3063, 3021 (m, aromatic C–H), 2922, 2862 (m, aliphatic C–H), 1598, 1588 (m, aromatic C=C), 1494, 1450 (s, aromatic C=C), 1250 (s, allyl C–S), 1127–1049 (s, C–O), 950 (m), 761 (m), 752 (m) cm⁻¹. Anal. Calcd for C₂₂H₂₈O₄S₂: C, 62.83; H, 6.71; S, 15.25. Found: C, 63.07; H, 6.64; S, 15.18%. ¹H NMR (300 MHz, CDCl₃, δ): 6.85–7.35 (m, 8H, aromatic), 4.19 (t, 4H, ArOCH₂), 4.01 (t, 4H, ArOCH₂CH₂), 3.85 (s, 4H, ArCH₂), 3.60 (t, 4H, OCH₂CH₂S), 2.65 (t, 4H, OCH₂CH₂S). ¹³C{¹H} NMR (75 MHz, CDCl₃) 156.5, 130.7, 128.3, 127.7, 121.3, 111.8, 70.7, 70.3, 68.3, 31.0, 30.0. Mass spectrum *m/z* (ESI): 420.6 [C₂₂H₂₈O₄S₂]⁺.

Preparation of [Pb(L²)(ClO₄)₂] (3). Pb(ClO₄)₂·3H₂O (16.4 mg, 0.036 mmol) in acetonitrile was added to a solution of L² (15.0 mg, 0.036 mmol) in dichloromethane (1 mL). Slow evaporation of the solution afforded an orange crystalline product 3 suitable for X-ray analysis. IR (KBr, pellet): 3070, 3028 (m, aromatic C–H), 2932, 2883 (m, aliphatic C–H), 1602, 1587 (m, aromatic C=C), 1495, 1452 (m, aromatic C=C), 1233 (m, allyl C–S), 1130–1103 (s, C–O), 1091 (s, ClO₄⁻), 1035 (s, C–O), 929 (m), 914 (m), 762(m), 627 (m), 619 (m) cm⁻¹. Anal. Calcd for C₂₂H₂₈O₁₂S₂PbCl₂: C, 31.96; H, 3.41; S, 7.76. Found: C, 32.05; H, 3.33 S, 8.07%. ¹H NMR (300 MHz,

CD₃CN, δ): 7.46–7.04 (m, 8H, aromatic), 4.52 (t, 4H, ArOCH₂), 4.26 (t, 4H, ArOCH₂CH₂), 4.50 (s, 4H, ArCH₂), 3.81 (t, 4H, OCH₂CH₂S), 3.24 (t, 4H, OCH₂CH₂S). Mass spectrum *m/z* (ESI): 726.9 [Pb(L²)(ClO₄)₂]⁺.

Caution! The perchlorate-containing complexes are potentially explosive and should be handled with great care.

Preparation of [Ag₂(L²)₂(NO₃)₂] (4). AgNO₃ (8.1 mg, 0.048 mmol) in methanol was added to a solution of L² (20.0 mg, 0.048 mmol) in dichloromethane (1 mL). Slow evaporation of the solution afforded a white precipitate. The precipitate was filtered off, washed with methanol and diethyl ether, and dried. Vapor diffusion of diethyl ether into DMF solution afforded a colorless crystalline product 4 suitable for X-ray analysis. mp 159–160 °C. IR (KBr, pellet): 3072, 3019 (m, aromatic C–H), 2923, 2868, 2838 (m, aliphatic C–H), 1598, 1584 (m, aromatic C=C), 1493, 1452 (m, aromatic C=C), 1401 (s, NO₃⁻), 1283, 1251 (s, allyl C–S), 1133–1103 (s, C–O), 1057 (m, C–O), 1018 (m), 936 (w), 768 (m), 745 (m) cm⁻¹. Anal. Calcd for C₄₄H₅₆Ag₂N₂O₁₄S₄: C, 44.75; H, 4.78; N, 2.37; S, 10.86. Found: C, 44.83; H, 4.75; N, 2.38; S, 10.84%. ¹H NMR (300 MHz, CD₃CN, δ): 7.34–6.91 (m, 8H, aromatic), 4.24 (t, 4H, ArOCH₂), 3.98 (t, 4H, ArOCH₂CH₂), 3.91 (s, 4H, ArCH₂), 3.33 (t, 4H, OCH₂CH₂S), 2.76 (t, 4H, OCH₂CH₂S). Mass spectrum *m/z* (ESI): 529.12 [Ag(L²)]⁺.

Preparation of [Cu(L²)] (5) and [(Cu₂I₂)(L²)₂] (6). CuI (4.6 mg, 0.024 mmol) and L² (10.0 mg, 0.024 mmol) were dissolved in acetonitrile. Slow evaporation of the solution afforded a mixture of colorless rhomboid- and brick-shaped single crystals. Under the microscope, the products were separated manually. The bulk purity for each part was confirmed by PXRD and identified through single-crystal X-ray analysis. The rhomboid-shaped crystals were [Cu(L²)] (5), and the brick-shaped crystals were [(Cu₂I₂)(L²)₂] (6).

For 5, mp 158–159 °C. IR (KBr, pellet): 3065, 3021 (m, aromatic C–H), 2935, 2885, 2872 (m, aliphatic C–H), 1599, 1586 (m, aromatic C=C), 1492, 1449 (s, aromatic C=C), 1252 (s, allyl C–S), 1136–1105 (s, C–O), 1049 (m), 1015(m), 944 (m), 753 (s) cm⁻¹. Anal. Calcd for C₂₂H₂₈I₁Cu₁O₄S₂: C, 43.25; H, 4.62; S, 10.49. Found: C, 43.06; H, 4.58; S, 10.72%. ¹H NMR (300 MHz, CD₃CN, δ): 7.35–6.93 (m, 8H, aromatic), 4.18 (t, 4H, ArOCH₂), 3.97 (t, 4H, ArOCH₂CH₂), 3.89 (s, 4H, ArCH₂), 3.65 (t, 4H, OCH₂CH₂S), 2.67 (t, 4H, OCH₂CH₂S). Mass spectrum *m/z* (ESI): 483.12 [CuL²]⁺.

For 6, mp 155–156 °C. IR (KBr, pellet): 3067, 3019 (m, aromatic C–H), 2923, 2907, 2864 (m, aliphatic C–H), 1598, 1586 (m, aromatic C=C), 1490, 1449 (s, aromatic C=C), 1249 (s, allyl C–S), 1133, 1106 (s, C–O), 1049 (m), 1019 (m), 940 (m), 751 (s) cm⁻¹. Anal. Calcd for C₄₄H₅₆I₂Cu₂O₈S₄: C, 43.25; H, 4.62; S, 10.49. Found: C, 43.05; H, 4.61; S, 10.74%. ¹H NMR (300 MHz, CD₃CN, δ): 7.35–6.93 (m, 8H, aromatic), 4.18 (t, 4H, ArOCH₂), 3.97 (t, 4H, ArOCH₂CH₂), 3.88 (s, 4H, ArCH₂), 3.64 (t, 4H, OCH₂CH₂S), 2.67 (t, 4H, OCH₂CH₂S).

Preparation of [Na₂(Cu₆I₈)(L²)₂(CH₃CN)₄]_n (7). A dichloromethane (1 mL) solution of L² (15.0 mg, 0.036 mmol) was allowed to diffuse slowly into an acetonitrile (1 mL) solution of CuI (27.2 mg, 0.144 mmol) and NaI (10.7 mg, 0.072 mmol) in a capillary tube (i.d. 5 mm). Slow evaporation of the solution afforded a colorless crystalline product 7 suitable for X-ray analysis. mp 164–165 °C. IR (KBr, pellet): 2923, 2907, 2864 (m, aliphatic C–H), 2268 (w, CN⁻), 1598, 1586 (m, aromatic C=C), 1490, 1449 (m, aromatic C=C), 1288 (w), 1238 (s, allyl C–S), 1092–1033 (s, C–O), 951 (m), 978 (m), 771 (m), 755 (m) cm⁻¹. Anal. Calcd for C₅₂H₆₈N₄O₈S₄Na₂Cu₆O₈: C, 25.51; H, 2.80; N, 2.29; S, 5.24. Found: C, 25.49; H, 2.77; N, 2.20; S, 5.12%.

X-ray Crystallographic Analysis. All data were collected on a Bruker SMART APEX2 ULTRA diffractometer equipped with graphite monochromated Mo K α radiation generated by a rotating anode. Data collection, data reduction, and semiempirical absorption correction were carried out using the software package APEX2.²⁶ All of the calculations for the structure determination were carried out using the SHELXTL package.²⁷ All hydrogen atoms were placed in idealized positions and refined isotropically in a riding manner along with their

respective parent atoms. Relevant crystal data collection and refinement data for the crystal structures are summarized in Table 1.

■ ASSOCIATED CONTENT

■ Supporting Information

TGA data for 7. Crystallographic data in CIF format. This material is available free of charge via the Internet at <http://pubs.acs.org>. CCDC 965568 (3), 989559 (4), 965569 (5), 965570 (6), and 965571 (7) contain the supplementary crystallographic data for this Paper. These data can be obtained free of charge from The Cambridge Crystallographic Data Center via www.ccdc.cam.ac.uk/data_request/cif.

■ AUTHOR INFORMATION

Corresponding Author

*E-mail: sslee@gnu.ac.kr.

Notes

The authors declare no competing financial interest.

■ ACKNOWLEDGMENTS

This work was supported by NRF (BRL-2012R1A4A1027750 and 2013R1A2A2A01067771).

■ REFERENCES

- (1) (a) Pedersen, C. J. *J. Am. Chem. Soc.* **1967**, *89*, 2495. (b) Lindoy, L. F. *The Chemistry of Macrocyclic Complexes*; Cambridge University Press: Cambridge, U.K., 1989. (c) Lehn, J.-M. *Supramolecular Chemistry, Concept and Perspectives*; VCH: Weinheim, Germany, 1995.
- (2) (a) Gale, P. A.; Steed, J. W. *Supramolecular Chemistry, From Molecules to Nanomaterials*; Wiley: Chichester, U.K., 2012. (b) Park, S.; Lee, S. Y.; Park, K.-M.; Lee, S. S. *Acc. Chem. Res.* **2012**, *45*, 391. (c) Levason, W.; Reid, G.; Zhang, W. *Dalton Trans.* **2011**, *40*, 8491. (d) Lindoy, L. F.; Park, K.-M.; Lee, S. S. *Chem. Soc. Rev.* **2013**, *42*, 1713.
- (3) (a) Lee, E.; Lee, S. S. *CrystEngComm* **2013**, *15*, 1814. (b) Lee, E.; Lee, S. S. *Inorg. Chem.* **2011**, *50*, 5803. (c) Kim, H. J.; Lee, S. S. *Inorg. Chem.* **2008**, *47*, 10807. (d) Farina, P.; Latter, T.; Levason, W.; Reid, G. *Dalton Trans.* **2013**, *42*, 4714. (e) Beattie, C.; Farina, P.; Levason, W.; Reid, G. *Dalton Trans.* **2013**, *42*, 15183. (f) Farina, P.; Levason, W.; Reid, G. *Dalton Trans.* **2013**, *42*, 89.
- (4) (a) Wolfe, S. *Acc. Chem. Res.* **1972**, *5*, 102. (b) Wolf, R. E., Jr.; Hartman, J. R.; Storey, J. M. E.; Foxman, B. M.; Cooper, S. R. *J. Am. Chem. Soc.* **1987**, *109*, 4328. (c) Blake, A. J.; Reid, G.; Schröder, M. *J. Chem. Soc., Chem. Comm.* **1992**, 1074. (d) Hill, S. E.; Feller, D. *J. Phys. Chem. A* **2000**, *104*, 652.
- (5) (a) Rottgers, T.; Sheldrick, W. S. *J. Solid State Chem.* **2000**, *152*, 271. (b) Rottgers, T.; Sheldrick, W. S. *Z. Anorg. Allg. Chem.* **2001**, *627*, 1976. (c) Heller, M.; Sheldrick, W. S. *Z. Anorg. Allg. Chem.* **2004**, *630*, 1869. (d) Heller, M.; Teichert, O.; Sheldrick, W. S. *Z. Anorg. Allg. Chem.* **2005**, *631*, 709. (e) Heller, M. *Z. Anorg. Allg. Chem.* **2006**, *632*, 441.
- (6) (a) Huang, D.; Zhang, X.; McInnes, E. J. L.; McMaster, J.; Blake, A. J.; Davies, E. S.; Wolowska, J.; Wilson, C.; Schröder, M. *Inorg. Chem.* **2008**, *47*, 91919. (b) Stephen, E.; Blake, A. J.; Carter, E.; Collison, D.; Davies, E. S.; Edge, R.; Lewis, W.; Murphy, D. M.; Wilson, C.; Gould, R. O.; Holder, A. J.; McMaster, J.; Schröder, M. *Inorg. Chem.* **2012**, *51*, 1450.
- (7) (a) Park, K.-M.; Yoon, I.; Seo, J.; Lee, J.-E.; Kim, J.; Choi, K. S.; Jung, O.-S.; Lee, S. S. *Cryst. Growth Des.* **2005**, *5*, 1707. (b) Lee, S. Y.; Park, S.; Kim, H. J.; Jung, J. H.; Lee, S. S. *Inorg. Chem.* **2008**, *47*, 1913. (c) Lee, S. Y.; Lee, S. S. *CrystEngComm* **2010**, *12*, 3471. (d) Park, I.-H.; Kim, H. J.; Lee, S. S. *CrystEngComm* **2012**, *14*, 4589.
- (8) (a) Seo, J.; Song, M. R.; Lee, J.-E.; Lee, S. Y.; Yoon, I.; Park, K.-M.; Kim, J.; Jung, J. H.; Park, S. B.; Lee, S. S. *Inorg. Chem.* **2006**, *45*, 952. (b) Lee, S. Y.; Jung, J. H.; Vittal, J. J.; Lee, S. S. *Cryst. Growth Des.* **2010**, *10*, 1033.
- (9) (a) Park, K.-M.; Seo, J.; Moon, S.-H.; Lee, S. S. *Cryst. Growth Des.* **2010**, *10*, 4148. (b) Kim, K.; Park, S.; Park, K.-M.; Lee, S. S. *Cryst. Growth Des.* **2011**, *11*, 4059. (c) Ju, H.; Lee, S. S. *Cryst. Growth Des.* **2012**, *12*, 4972.
- (10) (a) Blake, A. G.; Schröder, M. *Adv. Inorg. Chem.* **1990**, *35*, 1. (b) Loeb, S. J.; Shimizu, G. K. H. *Inorg. Chem.* **1993**, *32*, 1001. (c) Sultana, K. F.; Lee, S. Y.; Lee, J. Y.; Park, K.-M.; Lee, S. S. *Bull. Korean Chem. Soc.* **2008**, *29*, 241. (d) Yoon, I.; Seo, J.; Lee, J.-E.; Park, K.-M.; Kim, J. S.; Lah, M. S.; Lee, S. S. *Inorg. Chem.* **2006**, *45*, 3487. (e) Lee, S. Y.; Seo, J.; Yoon, I.; Kim, C.-S.; Choi, K. S.; Kim, J. S.; Lee, S. S. *Eur. J. Inorg. Chem.* **2006**, 3525.
- (11) Jin, Y.; Kim, H. J.; Lee, J. Y.; Lee, S. Y.; Shim, W. J.; Hong, S. H.; Lee, S. S. *Inorg. Chem.* **2010**, *49*, 10241.
- (12) (a) Heller, M.; Sheldrick, W. S. *Z. Anorg. Allg. Chem.* **2003**, *629*, 1589. (b) Lee, J. Y.; Lee, S. Y.; Park, S.; Kwon, J.; Shim, W.; Lee, S. S. *Inorg. Chem.* **2009**, *48*, 8934.
- (13) Atkins, I. M.; Lindoy, L. F.; Matthew, O. A.; Meehan, G. V.; Sobolev, A. N.; White, A. H. *Aust. J. Chem.* **1994**, *47*, 1155.
- (14) Nazarenko, A. Y.; Rusanov, E. B. *J. Coord. Chem.* **1995**, *34*, 265.
- (15) Shikazono, N.; Shimizu, M. *Can. Mineral.* **1992**, *30*, 137.
- (16) (a) Kim, H. J.; Song, M. R.; Lee, S. Y.; Lee, J. Y.; Lee, S. S. *Eur. J. Inorg. Chem.* **2008**, 3532. (b) Sague, J. L.; Meuwly, M.; Fromm, K. M. *CrystEngComm* **2008**, *10*, 1542.
- (17) (a) Drexler, H.-J.; Reinke, H.; Holdt, H.-J. *Chem. Ber.* **1996**, *129*, 807. (b) Blake, A. J.; Li, W.-S.; Lippolis, V.; Schröder, M. *Chem. Commun.* **1997**, *20*, 1943. (c) Blake, A. J.; Champness, N. R.; Howdle, S. M.; Morley, K. S.; Webb, P. B.; Wilson, C. *CrystEngComm* **2002**, *4*, 88.
- (18) (a) Knorr, M.; Pam, A.; Khatyr, A.; Strohmman, C.; Kubicki, M. M.; Rousselin, Y.; Aly, S. M.; Fortin, D.; Harvey, P. D. *Inorg. Chem.* **2010**, *49*, 5834. (b) Kim, T. H.; Shin, Y. W.; Jung, J. H.; Kim, J. S.; Kim, J. *Angew. Chem., Int. Ed.* **2008**, *47*, 685. (c) Peng, R.; Li, M.; Li, D. *Coord. Chem. Rev.* **2010**, *254*, 1.
- (19) Bondi, A. J. *Phys. Chem.* **1964**, *68*, 441.
- (20) (a) Kang, E.-J.; Lee, S. Y.; Lee, H.; Lee, S. S. *Inorg. Chem.* **2010**, *49*, 7510. (b) Jo, M.; Seo, J.; Lindoy, L. F.; Lee, S. S. *Dalton Trans.* **2009**, 6096. (c) Lee, S. Y.; Park, S.; Lee, S. S. *Inorg. Chem.* **2009**, *48*, 11335.
- (21) Paulsson, H.; Berggrund, M.; Fischer, A.; Kloos, L. Z. *Anorg. Allg. Chem.* **2004**, *630*, 413.
- (22) Bi, M.; Li, G.; Hua, J.; Liu, Y.; Liu, X.; Hu, Y.; Shi, Z.; Feng, S. *Cryst. Growth Des.* **2007**, *7*, 2066.
- (23) Ford, P. C. *Coord. Chem. Rev.* **1994**, *132*, 129.
- (24) (a) Vitale, M.; Palke, W. E.; Ford, P. C. *J. Phys. Chem.* **1992**, *96*, 8329. (b) Lee, J. Y.; Lee, S. Y.; Sim, W.; Park, K.-M.; Kim, J.; Lee, S. S. *J. Am. Chem. Soc.* **2008**, *130*, 6902. (c) Lee, J. Y.; Kim, H. J.; Jung, J. H.; Sim, W.; Lee, S. S. *J. Am. Chem. Soc.* **2008**, *130*, 13838.
- (25) (a) Vitale, M.; Ford, P. C. *Coord. Chem. Rev.* **2001**, *219*, 3. (b) Perruchas, S.; Goff, X. F. L.; Maron, S.; Maurin, I.; Guillen, F.; Garcia, A.; Gacoin, T.; Boilot, J.-P. *J. Am. Chem. Soc.* **2010**, *132*, 10967.
- (26) APEX2, Version 2009.1-0 Data Collection and Processing Software; Bruker AXS Inc.: Madison, WI, 2008.
- (27) SHELXTL-PC, (Version 6.22) Program for Solution and Refinement of Crystal Structures; Bruker AXS Inc.: Madison, WI, 2001.